Transmission Lines Loaded at Regular Intervals

SHASHI D. MALAVIYA, MEMBER, IEEE, AND V. P. SINGH

Abstract—**By a mathematical analysis, the switching time of an incident wave is predicted for a terminated net in which equal, lumped capacitive loads are repeated a finite number of times at regular intervals. The analysis is valid even for the case of only a few loads, for which the distributed load approximation is poor. An APL program has been developed to compute the delay; its use is demonstrated by an example. The results are extended to include complex loads.**

I. Introduction

INCIDENT wave switching is often required in high-speed electronic systems, involving intercommunication among several regularly spaced clusters of chips through printed wiring or conductors that are buried in the packaging. The conductors act as uniform transmission lines. Common examples are address and control lines feeding an array of memory chips, I/O lines between CPU's, etc. The lines usually end in matched terminators to suppress unwanted reflections. Every connection to a chip imposes a load on the transmission line which can generally be treated as a lumped capacitance shunted by a resistance. This is particularly true of high-speed current switch circuits, for which the load consists of one or more bases of current switches. Typically, such loads are spaced several inches apart. The propagation delay in such cases is calculated by the following popular approximation [1]:

$$T_L = T_0(1 + C_L/C_0)^{1/2} \text{ ns per unit length} \qquad (1)$$

where

T_L loaded delay,
T_0 unloaded delay,
C_L load capacitance per unit length of the line,
C_0 unloaded line capacitance per unit length.

As will be seen later, the approximation given in (1) is too crude in many practical situations. In this paper, we have developed a more accurate closed-form solution for calculating the propagation delay of the incident wave. However, the expressions derived here apply only to the incident wave and do not take into account subsequent internal reflections. Also, this analysis is only valid for linear, equally spaced identical loads.

In most of the high-speed systems, the incident wave itself is required to switch the circuits, without waiting for the subsequent reflections. The subsequent reflections can, therefore, be ignored, except in the cases where they are so large as to cause false switching. This situation is generally avoided by proper far-end termination and by placing restrictions on the number, spacing, and magnitude of loads permitted on any line.

For two practical cases of step and ramp inputs, we have developed analytical expressions for the final output voltage in terms of the incomplete gamma functions. Apart from being more accurate, our approach is easily programmable. Another advantage of this approach is that the effects of finite switching times of the input signals are also accounted for, and the user can pick the desired level (e.g., 90 or 95 percent of the final) up to which he wants to calculate the delay.

Since only the forward wave is of interest in such cases, ignoring the rereflected waves simplifies the analysis very considerably. Furthermore, in practical situations involving, for example, six stubs, the rereflected waves are highly attenuated by the time they reach the last load, except for the one that rebounds between the last and next to last loads. Since the nodes have negative reflection coefficients, the rereflected waves add positively with the incident wave. By ignoring the rereflected waves, therefore, we err on the safe side. The analysis also implies that the stubs are well separated from each other so that the outgoing wave reaches its final value before encountering the next stub. The delay will increase if the stubs are brought closer together. The delay in the extreme case, when the spacing between the loads approaches zero, is easily calculated by our approach.

Finally the total delay computed by using our approach is compared with that of the approximation in (1), as well as with the actual delay obtained from ASTAP [4].

II. Analysis

Fig. 1 shows a uniform line with C pF at intervals of L cm, giving a total capacitive load of nC pF for n such loads. The far end of the line is terminated into Y_0 which is the characteristic admittance of the unloaded line. In this analysis, we assume that the line constants Y_0, τ, and C, etc., are "effective" values, almost constant over the frequency range of interest so that their Laplace transforms are independent of s. Let a positive-going voltage wave $V(s)$ be incident upon the line. The reflection coefficient $\rho(s)$ is given by

$$\rho(s) = \frac{Y_0 - Y_L}{Y_0 + Y_L} \qquad (2)$$

Manuscript received October 21, 1977; revised September 7, 1978.
The authors are with IBM System Products Division, East Fishkill, Hopewell Junction, NY 12533.

0018-9480/79/1000-0854$00.75 ©1979 IEEE

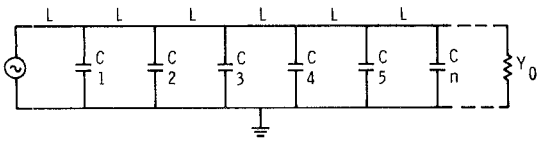

Fig. 1. Transmission-line network, C given in picofarads.

where, neglecting rereflections

$$Y_L = Y_0 + sC. \tag{3}$$

The transmission coefficient $T(s)$ is given by

$$T(s) = 1 + \rho(s) = \frac{a}{s+a} \tag{4}$$

where

$$a = 2Y_0/C. \tag{5}$$

The forward-going wave, after passing through all the n sections (or stubs) is given by (again neglecting rereflections)

$$V_{out}(s) = \left(\frac{a}{s+a}\right)^n V_{in}(s) e^{-n\tau s} \tag{6}$$

where τ is the delay per section and $V_{in}(s)$ is the Laplace transform of the input wave.

In (6), the term $e^{-n\tau s}$ represents the propagation delay of the unloaded line through all the n stubs. Since the computation of this delay is straightforward, we ignore it initially and compute the degradation in the switching time of the forward-going wave as it passes through the loads. The total switching delay is then computed by adding the propagation delay to the degraded switching time. The degraded switching time is calculated from (6) by dropping the propagation delay term from it. Therefore, (6) reduces to

$$V_{out}(s) = \left(\frac{a}{s+a}\right)^n V_{in}(s). \tag{7}$$

This equation is strictly valid for the forward-going wave. However as explained in the introduction, it can also be used for computing the incident switching delays of high-speed nets, consisting of a driver and a terminated transmission line loaded at regular intervals with equal linear loads. We shall use (7) in obtaining closed-form solutions for step and ramp inputs.

III. Step Input

For a step input

$$V_{in}(s) = A/s \tag{8}$$

where A is the amplitude of the step. Substituting (8) in (7) gives

$$V_{out}(s) = \frac{Aa^n}{s(s+a)^n}. \tag{9}$$

The inverse transform of (9) is, therefore, given by

$$V_{out}(t) = \frac{A}{(n-1)!}\int_0^{at} x^{n-1}e^{-x}\,dx \tag{10}$$

$$= AP(n,at) \tag{11}$$

TABLE I
Values of n and x for The Most Commonly Needed Values of $P(n,x)$

n	x P(n, x) = 0.90	P(n, x) = 0.95
1	2.4	3.0
2	3.9	4.8
3	5.4	6.3
4	6.7	7.8
5	8.1	9.2
6	9.3	10.6
7	10.5	12.0
8	11.9	13.4
9	13.0	14.8
10	14.2	15.8

where

$$P(n,x) = \frac{1}{(n-1)!}\int_0^x t^{n-1}e^{-t}\,dt = 1 - e^{-x}\sum_{r=0}^{n-1}\frac{x^r}{r!}. \tag{12}$$

Equation (12) defines an incomplete gamma function, whose values are tabulated in [2], [3]. The delay T_R, in reaching 90 percent (or 95 percent) of the final value, is given in Table I.

The total switching delay T_D is given by

$$T_D = T_\rho + T_R \tag{13}$$

where

- T_D switching delay for reaching a specified percentage (e.g., 90 or 95 percent) of the final level,
- T_ρ total propagation delay through the n sections,
- T_R rise or fall time up to the desired voltage level (generally the switching threshold) of the forward-going wave after passage through the loaded line.

The input voltage, being a step function, has zero rise or fall time.

IV. Ramp Input

As shown in Fig. 2(a), a voltage ramp starting with a delay δ_1 and with slope K is given by

$$V'_{in}(t) = KtU(t-\delta_1). \tag{14}$$

If it is to level off after a total delay of δ_2, we must add another ramp, as shown in Fig. 2(b):

$$V''_{in}(t) = -KtU(t-\delta_2). \tag{15}$$

The final input is, therefore, as shown in Fig. 2(c):

$$V_{in}(t) = Kt[\,U(t-\delta_1) - U(t-\delta_2)\,]. \tag{16}$$

The Laplace transform of $V_{in}(t)$ is

$$V_{in}(s) = (K/s^2)[\exp(-\delta_1 s) - \exp(-\delta_2 s)]. \tag{17}$$

The output voltage is given by substituting (17) in (7):

$$V_{out}(s) = \frac{Ka^n}{s^2(s+a)^n}[\exp(-\delta_1 s) - \exp(-\delta_2 s)] \tag{18}$$

$$= V_{out1}(s) - V_{out2}(s) \tag{19}$$

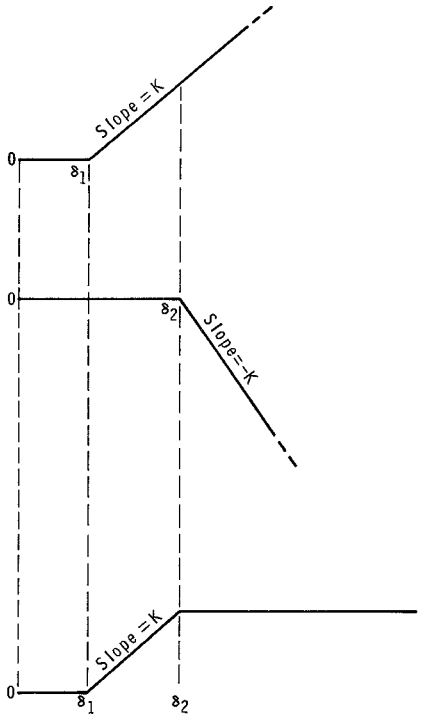

Fig. 2. Ramp input waveforms.

where

$$V_{out1}(s) = \frac{Ka^n}{s^2(s+a)^n}\exp(-\delta_1 s) \tag{20}$$

and

$$V_{out2}(s) = \frac{Ka^n}{s^2(s+a)^n}\exp(-\delta_2 s). \tag{21}$$

Since the two expressions are identical except for the constants δ_1 and δ_2, the solution of $V_{out1}(s)$ will also give the solution of $V_{out2}(s)$.

Solution for $V_{out1}(t)$:

Let

$$F_1(s) = \frac{a^n}{(s+a)^n}$$

and

$$F_2(s) = (1/s^2)\exp(-\delta_1 s).$$

The corresponding inverse transforms are given by

$$f_1(t) = \frac{a^n t^{n-1} e^{-at}}{(n-1)!}$$

and

$$f_2(t) = (t-\delta_1)\,U(t-\delta_1).$$

Using the convolution theorem

$$F(t) = \int_0^t f_1(t-y) f_2(y)\,dy$$

we have

$$F(t,\delta_1) = a^n \int_0^t \frac{(t-y)^{n-1}}{(n-1)!} e^{-a(t-y)}(y-\delta_1)\,U(y-\delta_1)\,dy$$

$$= \frac{a^n}{(n-1)!}\int_{\delta_1}^t (t-y)^{n-1} e^{-a(t-y)}(y-\delta_1)\,dy, \qquad t>\delta_1. \tag{22}$$

Let $x = a(t-\delta_1)$; then

$$F(t,\delta_1) = \frac{1}{(n-1)!}\left[\frac{x}{a}\int_0^x y^{n-1}e^{-y}\,dy - \frac{1}{a}\int_0^x y^n e^{-y}\,dy\right]$$

$$= \frac{x}{a}P(n,x) - \frac{n}{a}P(n+1,x) \tag{23}$$

where $P(n,x)$ is defined in (12).

Using the recurrence relation for incomplete gamma functions [3]

$$P(n+1,x) = P(n,x) - \frac{x^n}{n!}e^{-x} \tag{24}$$

we can write (23) as follows:

$$F(t,\delta_1) = \frac{x-n}{a}P(n,x) - \frac{n}{a}\frac{x^n}{n!}e^{-x}. \tag{25}$$

Now, using (20) and (25), we get

$$V_{out1}(t) = KF(t,\delta_1). \tag{26}$$

A similar expression can be developed for (21):

$$V_{out2}(t) = KF(t,\delta_2) \tag{27}$$

where $F(t,\delta_2)$ is obtained from (22) and (25) by replacing δ_1 with δ_2. Finally, combining (19), (26), and (27), we get

$$V_{out}(t) = K[F(t,\delta_1) - F(t,\delta_2)]. \tag{28}$$

Thus $V_{out}(t)$ is expressed in terms of incomplete gamma functions. It can be evaluated directly from (28) as a function of time from which the switching time up to the desired output level is easily obtained as shown in the following example.

Example: For the following input parameters:

Load capacitance	10 pF
Number of loads	4
Rise/fall time	6.0 ns
Final voltage level	2.0 V
Characteristic impedance	70 Ω.

The $V_{out}(t)$ as a function of time is

0(0), 0(0.2), 0.001(0.4), 0.005(0.6), 0.014(0.8), 0.032(1), 0.057(1.2), 0.091(1.4), 0.132(1.6), 0.18(1.8), 0.233(2), 0.289(2.2), 0.349(2.4), 0.41(2.6), 0.474(2.8), 0.538(3), 0.603(3.2), 0.669(3.4), 0.735(3.6), 0.801(3.8), 0.867(4), 0.934(4.2), 1(4.4), 1.07(4.6), 1.13(4.8), 1.2(5), 1.27(5.2), 1.33(5.4), 1.4(5.6), 1.47(5.8), 1.53(6), 1.6(6.2), 1.67(6.4), 1.73(6.6), 1.79(6.8), 1.84(7), 1.88(7.2), 1.91(7.4), 1.93(7.6), 1.95(7.8), 1.97(8), 1.98(8.2), 1.98(8.4), 1.99(8.6), 1.99(8.8), 2(9), 2(9.2), 2(9.4), 2(9.6), 2(9.8), 2(10), $\cdots$, 2(15).

In the above example time t was taken in the interval [0, 15] in steps of 0.2 ns. For each V_{out} value, the time t is given in the parentheses.

V. Complex Loads

Let the load consist of $G+sC$. Equations (3) and (4) are then modified to

$$Y_L = Y_0 + G + sC \tag{29}$$

and

$$T(s) = \frac{a}{s+a'} \tag{30}$$

where

$$a' = a + G/C. \tag{31}$$

Equation (7) can now be expressed as

$$V_{out}(s) = \frac{a}{a'} \frac{a'}{s+a'} V_{in}(s). \tag{32}$$

The effect of adding a shunt conductance G to the load is, therefore, accounted for by multiplying the final output by the factor a/a' and replacing a with a' throughout the rest of the analysis.

VI. Computations of the Final Voltage Output

An APL program is written to evaluate the final output voltage on the line as a function of time. In this program we ignore rereflected waves in computing the output. We presume that the far end of the line is terminated in its characteristic impedance and that the stubs on the line are well separated from each other, so that the voltage can attain its final value before encountering the next stub. Each stub is represented by a lumped capacitance of 10 pF. Fig. 3 gives results for 1–6 stubs on the line.

To show the effect of closer spacing of the stubs, the extreme case of zero spacing between the stubs is also worked out here; the results are given in Fig. 4. Clustering N stubs together corresponds to a single stub with a load of $10N$ pF. These results have been obtained from the same general program by putting $N=1$ and $C=10N$. Using the figures, we can find the output rise time for N well-separated stubs on the line (with 10 pF per stub) and compare it with the corresponding rise time for a single stub with $10N$ pF load.

Table II gives the two rise times and their difference for $N=1$ through $N=6$. Input rise time in this case is 2 ns. Capacitive loading per stub was kept the same.

VII. Total Switching Delays

We now compute the total switching delay T_D, given in (13) for widely separated loads. This delay is calculated by using three different methods, viz., popular approximation

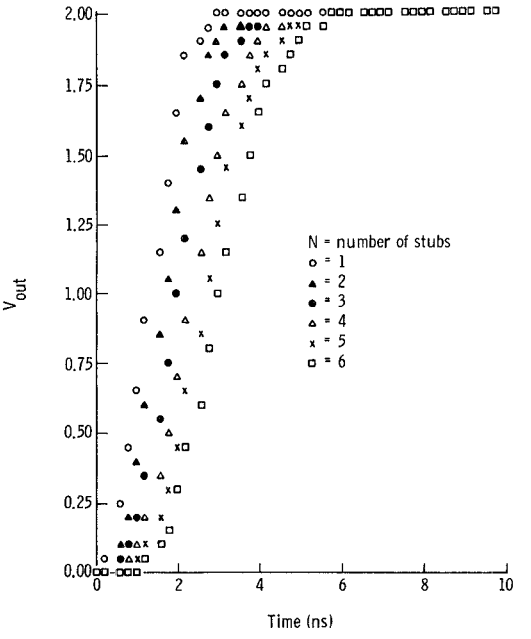

Fig. 3. Output voltage versus time for a load of 10 pF/stub. Input rise time, 2 ns.

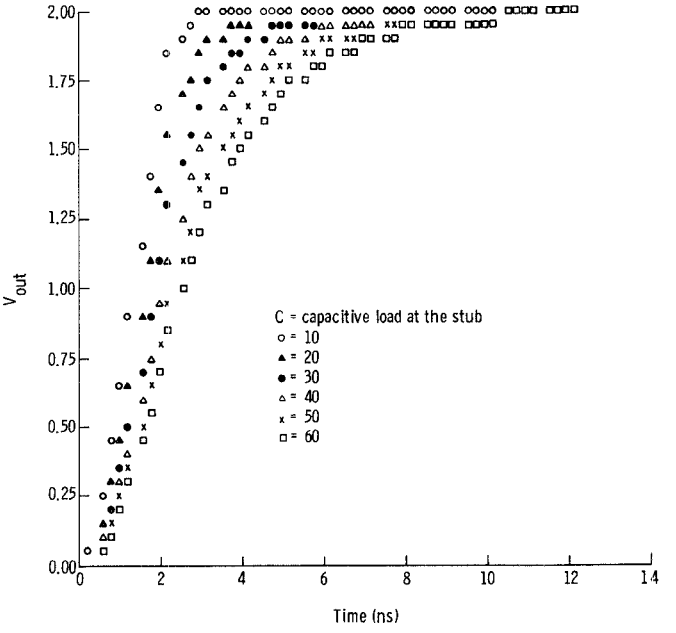

Fig. 4. Output voltage versus time, for a single stub. Input rise time, 2 ns.

TABLE II
Output Rise Time for Stub Spacing; Input Rise Time, 2 ns

Number of Stubs	Stubs Lumped Together	Stubs Widely Separated	Difference
1	3.50	3.50	0
2	5.50	4.25	1.25
3	7.50	5.00	2.50
4	9.75	5.50	4.25
5	11.75	6.25	5.50
6	13.75	6.75	7.00

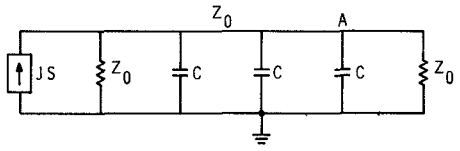

Fig. 5. Transmission line with three widely separated loads.

given in (1), our closed-form solution given in (28), and the ASTAP method [4].

A. Widely Separated Loads

Fig. 5 shows a transmission line driven by a matched source and terminated in its characteristic impedance Z_0 at the far end. It is tapped with three equal capacitive loads at regular intervals.

To illustrate the relative errors between the distributed load approximation and the results derived in this paper, we use the following example:

Line delay (unloaded)	$T_0 = 0.129$ ns/cm
Characteristic impedance	$Z_0 = 90\ \Omega$
Capacitance per load	$C = 20$ pF
Total number of loads	$N = 3$
Spacing between loads	$L = 20$ cm
Incident wave voltage	$V = 2$ V
Input ramp rise time	$T_R = 1$ ns
Switching threshold of the receiver (percentage of final level)	= 90 percent

Uniformly Distributed Load Approximation: As stated in the introduction, the loaded delay from (1) is

$$T_L = T_0\left(1 + \frac{C_L}{C_0}\right)^{1/2}.$$

The unloaded line capacitance per unit length is

$$C_0 = \frac{T_0}{Z_0} = \frac{0.129}{0.09} = 1.43 \text{ pF per cm.}$$

The load capacitance per unit length is

$$C_L = \frac{C}{L} = 1.0 \text{ pF per cm.}$$

Therefore, the loaded delay is

$$T_L = 0.129\left(1 + \frac{1}{1.43}\right)^{1/2} = 0.168 \text{ ns/cm.}$$

Total propagation delay to the last load (node 'A') is

$$T_p = 3 \cdot T_L \cdot L = 10.08 \text{ ns.}$$

With uniform load distribution, there is no distortion of the input waveform and the rise time at the load, therefore, remains equal to the incident rise time T_R, which for 90-percent threshold means an additional delay of 0.9 ns. The total switching delay is, therefore, given by

$$T_s = T_p + (90 \text{ percent of } T_R) = 10.98 \text{ ns.}$$

Forward Wave Approximation: Using (28), for $N = 3$ we find that the rise-time delay to 90-percent level (1 V) is 5.32 ns. To this we add the unloaded propagation delay to the last node 'A' (7.74 ns). It gives a total switching delay of 13.06 ns, according to the technique presented in this paper.

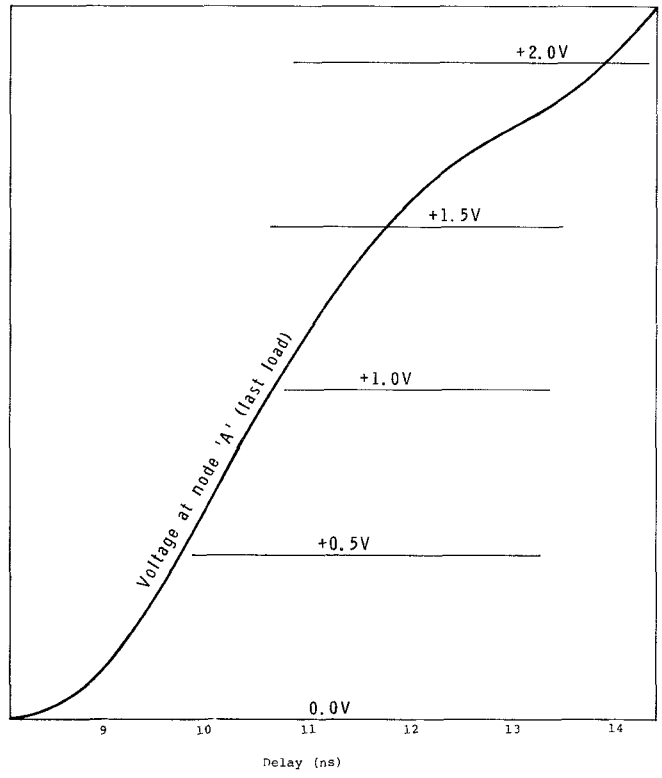

Fig. 6. ASTAP output.

Actual Delay: The actual waveshape, as obtained by the ASTAP computer analysis, is shown in Fig. 6. The switching delay to a 90-percent level is seen to be 13.07 ns. The ASTAP program is valid for close, as well as widely separated, equal or unequal complex loads. It takes into account all the internal and end point reflections in its computations.

B. Other Examples

Following the procedure outlined in Section VII-A, the total delays in few other cases, computed by three different methods for thresholds ranging from 10 to 95 percent, are given in the following examples.

EXAMPLE 1:

PARAMETERS OF THE NET

C	N	TR	V	Z0	T0	L
80	1	2	2	0.09	0.129	100

PERCENT LEVEL	TOTAL DELAY: POP. APPROX.	OUR METHOD	ASTAP (ACTUAL)
10	16.302	14.17	14.166
50	17.102	16.442	16.468
90	17.902	22.236	22.258
95	18.002	24.731	24.754

EXAMPLE 2:

PARAMETERS OF THE NET

C	N	TR	V	Z0	T0	L
60	1	1	2	0.09	0.129	60

PERCENT LEVEL	TOTAL DELAY: POP. APPROX.	OUR METHOD	ASTAP (ACTUAL)
10	10.185	8.5085	8.508
50	10.585	10.127	10.16
90	10.985	14.473	14.495
95	11.035	16.344	16.365

EXAMPLE 3:

PARAMETERS OF THE NET

C	N	TR	V	Z0	T0	L
20	2	1	2	0.09	0.129	20

PERCENT LEVEL	TOTAL DELAY: POP. APPROX.	OUR METHOD	ASTAP (ACTUAL)
10	6.8232	6.0836	6.081
50	7.2232	7.1894	7.3
90	7.6232	9.1959	9.306
95	7.6732	9.966	10.119

EXAMPLE 4:

PARAMETERS OF THE NET

C	N	TR	V	Z0	T0	L
20	3	1	2	0.09	0.129	30

PERCENT LEVEL	TOTAL DELAY: POP. APPROX.	OUR METHOD	ASTAP (ACTUAL)
10	14.153	13.061	13.056
50	14.553	14.528	14.566
90	14.953	16.929	16.952
95	15.003	17.808	17.822

EXAMPLE 5:

PARAMETERS OF THE NET

C	N	TR	V	Z0	T0	L
20	2	2	2	0.09	0.129	100

PERCENT LEVEL	TOTAL DELAY: POP. APPROX.	OUR METHOD	ASTAP (ACTUAL)
10	27.741	27.023	27.018
50	28.541	28.381	28.398
90	29.341	30.436	30.446
95	29.441	31.212	31.207

EXAMPLE 6:

PARAMETERS OF THE NET

C	N	TR	V	Z0	T0	L
20	3	1	2	0.09	0.129	20

PERCENT LEVEL	TOTAL DELAY: POP. APPROX.	OUR METHOD	ASTAP (ACTUAL)
10	10.185	9.1907	9.188
50	10.585	10.658	10.695
90	10.985	13.059	13.072
95	11.035	13.938	13.612

VIII. Conclusion

The approach presented in this paper gives a more accurate closed-form solution (28) for incident switching delays than the popular loaded-line delay approximation given in (1). A glance at the comparative results given in the previous section gives an idea of the errors involved under different loading and switching conditions. It should be noted that the increase in delay due to close spacing of loads is not properly accounted for in this approximation, the solution being exact only for widely separated loads. Table II shows how the delay increases when the stub spacing is reduced to zero (all the loads lumped together).

Apart from being more accurate for a large number of high-speed switching nets, the technique presented here is easy to apply. However it should be used only where multiple rereflections between the loads can be ignored.

Acknowledgment

The authors are grateful to the reviewers' comments which resulted in substantially improving the original draft of this paper.

References

[1] Joseph L. DeClue, "Wiring for high speed circuits," *Electron. Design*, vol. 24, no. 11, pp. 84–86, May 24, 1976.

[2] S. M. Selby, (Ed.), *Standard Mathematical Tables*. (15th ed.), 1967, pp. 546–551.

[3] M. Abramowitz and I. A. Stegun, (Eds.), *Handbook of Mathematical Functions*. National Bureau of Standards, AMS 55, 1964, pp. 260–262, pp. 978–985.

[4] *Advanced Statistical Analysis Program* (ASTAP). program no. 5796-PBH, manual no. SH20-1118-0, IBM Corporation.